Available online at www.sciencedirect.com
SCIENCE DIRECT
Colloids and Surfaces A: Physicochem. Eng. Aspects 282–283 (2006) 387–401
COLLOIDS AND SURFACES A
www.elsevier.com/locate/colsurfa

On the equation of the maximum capillary pressure induced by solid particles to stabilize emulsions and foams and on the emulsion stability diagrams

G. Kaptay

Department of Chemistry, Faculty of Materials Science and Engineering, University of Miskolc, H-3515 Miskolc, Egyetemvaros, Hungary

Received 2 October 2005; received in revised form 7 December 2005; accepted 12 December 2005
Available online 19 January 2006

Dedicated to Professor Ivan B. Ivanov (LCPE, University of Sofia) on the occasion of his 70th birthday.

Abstract

The knowledge of the adequate equation for the maximum capillary pressure ($P_c^{\max}$), stabilizing relatively large bubbles and drops by relatively small, solid particles, is essential to control the stability of foams and emulsions. The idea to introduce this quantity to explain emulsion stability was published in the break-through paper by professor I.B. Ivanov and his co-workers [N.D. Denkov, I.B. Ivanov, P.A. Kralchevsky, D.T. Wasan, A possible mechanism of stabilization of emulsions by solid particles, J. Colloid Interface Sci. 150 (1992), 589–593]. A higher positive value of $P_c^{\max}$ ensures that a thin liquid film between the droplets (of an emulsion), or between the bubbles (of a foam) can withstand a higher pressing force. In the present paper, different equations for $P_c^{\max}$ are reviewed, published since the above cited paper. The exact form of this equation depends on the arrangement of particles in the liquid film between the drops (in the case of emulsions) or between the bubbles (in the case of foams). In the present paper the following general equation is derived for the maximum capillary pressure: $P_c^{\max} = \pm 2p\sigma(\cos\theta \pm z)/R$, with a '+' sign, referring to o/w emulsions and foams, and with a '−' sign, referring to w/o emulsions; R, the radius of the spherical solid particle; σ, the interfacial energy between the two liquids (in case of emulsions), or between the liquid and gas (in case of foams); θ, the contact angle of the water droplet in the environment of the oil phase on the solid particle (in case of emulsions) or of the liquid in gas phase on the solid particle (in case of foams), parameters p and z are functions of particle arrangement. Particularly, $z = 0$ for the single layer of particles, and $z = 0.633$ (at $\theta > 90^\circ$) for the closely packed double layer of particles. The above equation was jointly analyzed with the well-known equation for the energy of removal of the particles from the liquid/liquid interface. As a result, emulsion stability diagrams (ESD) have been created with the contact angle and volume fraction of the water phase on its axes, indicating the stability intervals for o/w and w/o emulsions. The emulsion stability diagram was used to explain the phenomenon of 'catastrophic phase inversion' (i) due to solely changing the volume fraction of water, and (ii) due to solely changing the particle concentration, in the system of the same composition (water, oil, solid). The emulsion stability diagram was also used to rationalize the transitional phase inversion due to changing the ratio of hydrophobic to hydrophilic particles as function of water content. Stabilization of emulsions and foams by a 3D network of solid particles is also discussed.

Keywords: Emulsions; Foams; Stabilization; Solid particles; Capillary pressure; Phase inversion; Emulsion stability diagram; Pickering emulsion

1. Introduction

On 18 June, 1903 a lecture was read by W. Ramsden at the Royal Society [1], showing that 'the persistence of many emulsions is determined by the presence of solid matter at the interfaces of the two liquids, and that the solid matter at the interfaces of the above emulsion-pairs occurs because the surface energy is thereby diminished'. Several years later, Pickering [2] realized, that oil-in-water emulsions form only, if 'the solids are wetted more easily by water than by oil, otherwise there is no emulsification at all'. Five years later, after fully (!) quoting and critically analyzing Pickering's paper, Bancroft [3] made the following conclusion: "a corollary of his hypothesis is that insoluble particles, which are more readily wetted by oil than by water, should tend to promote the emulsification of water in oil". Based on Bancroft's hypothesis, and under the supervision of Briggs, Newman was probably the first, who was able to stabilize water-in-oil emulsions by solid particles [4]. By the year of 1921, sufficient experimental evidence was collected

E-mail addresses: kaptay@hotmail.com, fkmkap@uni-miskolc.hu.

0927-7757/$ – see front matter © 2005 Elsevier B.V. All rights reserved.
doi:10.1016/j.colsurfa.2005.12.021

to distinguish between the conditions to form oil-in-water and water-in-oil emulsions, so Briggs was able to write [5]: 'It is generally agreed that the liquid which wets the solid emulsifier the more strongly under the conditions of the experiment, tends to become the outside phase, the less strongly wetting liquid being broken up into drops. Just why this is so is difficult to explain satisfactorily for the moment'. This question was answered in two papers by Hildebrand et al. by claiming that 'if there are enough solid particles to fill the interface the tendency of the interface to contract will cause it to bend in the direction of the more poorly wetting liquid, which makes it easy for the latter to become the enclosed phase' [6], and later: 'in forming the emulsion droplets having the particles chiefly on the outside of the interface would be better protected from coalescing than those having the particles more in the inside' [7]. In the latter paper, the first microphotographs of emulsions stabilized by solid particles for both o/w and w/o emulsions were published. The final experimental confirmation of this hypothesis was presented by the series of experiments by Schulmann and Leja [8], who also tailored the condition further as: (i) o/w emulsions are stabilized by solid particles, if the contact angle is slightly less than 90° (measured through the water phase), and (ii) w/o emulsions are stabilized by solid particles, if the contact angle is slightly more than 90°. The further literature on solid particle stabilized liquid foams and emulsions is summarized in the number of reviews during the last decade [9–18].

One could expect that based on the widely known and accepted works of Young and Laplace on wettability and capillary pressure (100 years before the pioneering works of Ramsden and Pickering) the above statements would be translated into mathematical equations relatively soon and be accepted smoothly. However, it was not the case, mostly because two, partly contradicting each other equations are needed to describe the stabilization of emulsions by solid particles. From the one hand, the particles must be stable at the interface to stabilize emulsions (the need for the first equation). On the other hand, the particles must stabilize the thin liquid film, separating large bubbles or droplets (the need for the second equation).

The condition of stability of a solid particle at a liquid/liquid interface is most often described in the emulsion-literature by the energy, requested to remove the particle from its equilibrium position at the interface to the bulk liquid phases:

$$\Delta G_{\text{remove}} = \pi R^2 \sigma (1 \pm \cos \Theta)^2 \quad (1)$$

where R is the radius of the spherical solid particle; σ, the interfacial energy between the two liquids (in case of emulsions), or between the liquid and gas (in case of foams); Θ (i) the contact angle, measured through the water phase on a solid particle in the environment of the oil phase (in case of emulsions) or (ii) the contact angle of the liquid phase (water, oil, liquid metal, or whatever liquid is foamed) on a solid particle in gas environment (in case of foams); sign '+' refers to particle removal into the bulk oil phase (in case of emulsions) or into the gas phase (in case of foams), while sign '−' refers to the removal of the particle into the bulk water phase (in case of emulsions) or into the liquid phase (in case of foams).

Eq. (1) was re-invented independently in the literature several times. It was derived independently by Koretzki and Kruglyakov [19], by Scheludko et al. [20], by Tadros and Vincent [21], by Levine et al. [22], by Clint and Taylor [23] and by Tambe and Sharma [24]. Among these 'original' papers [19,20,24] were never cited for Eq. (1) in the emulsion literature. On the other hand, Ref. [21] was cited by Ref. [25], Ref. [22] was cited by Refs. [16,26–28], Ref. [23] was cited by Refs. [29–32]. Eq. (1) was further improved to take into account the curvature of the droplet interface [33,34], and also the line tension and monolayer curvature (bending) energy [16,35–37]. For similar purposes, the maximum force, keeping the particle at the liquid/gas interface (as the first condition to stabilize foams) was described independently by the author [38]. History beside, the physical meaning of Eq. (1) is more important. From this equation one can make the following conclusions:

(i) the particle will be stable at the liquid/liquid interface only, if the contact angle is significantly larger than 0°, but significantly lower than 180°;
(ii) the highest stability of the particle at the liquid/liquid interface will take place when the contact angle equals 90°;
(iii) many authors stated that once the particles are stabilized at the liquid/liquid interface, they will inevitably stabilize emulsions. Therefore, it is essential to underline here that this conclusion does not follow from Eq. (1).

Despite the obvious success of Eq. (1) in the emulsion literature, it is unable to explain the detailed observations, made first by Schulmann and Leja [8] (see above), who claimed that for the highest stabilization of emulsions the contact angle should be somewhat different from 90°. This observation was further confirmed by the studies [26,39–42] (see also Ref. [76] in [15]). Most importantly, Eq. (1) does not say anything about the stability of the thin liquid layer between large droplets (bubbles), which are stabilized by the particles. This gap in our understanding (i.e. 'why particles are stable at liquid/liquid interfaces' (answered by Eq. (1)) and 'why a thin liquid layer is stable between the droplets or bubbles' (not answered by Eq. (1))) was first realized by professor I.B. Ivanov and co-workers. As a result, the first paper, introducing the 'maximum capillary pressure', being responsible for the stability of the thin liquid film between the droplets of the emulsion was published by Denkov et al. [43] with the following equation:

$$P_c^{\max} = p^* \frac{2\sigma}{R} \quad (2)$$

where p^* is a parameter with a positive value, being the function of interface coverage by particles, particle arrangement in the thin liquid film and contact angle.

A higher positive value of $P_c^{\max}$ ensures that a thin liquid film between the droplets (of an emulsion), or between the bubbles (of a foam) can withstand a higher pressing force. From Eq. (2) one can conclude that the thin liquid film between the droplets or bubbles will be stronger when the interfacial energy will be higher and the size of the particles will be lower. However, these consequences follow also from Eq. (1), at least, for a unit volume

of particles. A significantly new information, contained in Eq. (2) is hidden in parameter p^*. Although from numerical values of parameter p^*, given in [43] one can make the conclusion that the stability of the film will be highest at the contact angle of 0°, and it will become zero at the contact angle of 90°, the dependence of parameter p^* on the contact angle was not written by an explicit equation in [43]. Probably this is the main reason why Eq. (2) was not re-written in the majority of independent citing papers [9,11,16,18,25,27,35,36,44–62], unlike Eq. (1). Thus, Eqs. (1) and (2) have not been confronted or treated jointly in the literature, except in the papers of the present author [38,63–65].

A similar equation was later independently derived for a single layer of particles in [45] and later in [38][1] (see also [63–66]). Eq. (2) was developed further [55] for the closely packed double layer of particles. This and further particle configurations were considered in [38].

In the present paper all equations, developed so far in the literature on the maximum capillary pressure, stabilizing thin liquid films by solid particles will be reviewed and discussed. The maximum capillary pressure will be expressed as the function of contact angle in the explicit way and Eqs. (1) and (2) will be analyzed together.

2. Equations for P_c^{max} for a single layer of particles

A single layer of particles at the liquid/liquid interface is a most obvious and simple model for the stabilization of emulsions by solid particles. The first schematic picture of this type was given by Finkle et al. [6] (see also [67], and others). The images of closely packed single layer of particles at oil/water interface [15,22] and at water/air interface [68] were presented by different techniques. The closely packed layer was shown to appear due to the attraction between the particles [69]. The hexagonally ordered monolayer of particles was observed by confocal microscopy at the oil/water interface [70] (see also [46,71]). A 2D flocculated single layer of particles (with surface coverage of $f = 0.29$) was found to be sufficient to stabilize emulsion [72].

2.1. The method and results of Denkov et al. [43]

The first equation to describe the interfacial pressure, separating two, relatively large drops by relatively small solid spherical particles of equal size, was published by Denkov et al. [43]. In this model, the solid particles are supposed to form a single layer between the two droplets. In fact, only the surrounding of one particle is analyzed, without the influence of the neighboring particles, what is the main simplification of this model. It is supposed that each particle of radius R is responsible for the stability of a circular area of radius b of the liquid/liquid interface (see Fig. 1). The running radius, drawn to the liquid/liquid interface is denoted by r (Fig. 1). By introducing the dimensionless parameters: $b^* = b/R$ and $r^* = r/R$ into Eqs. (2.1)–(2.10) of [43]

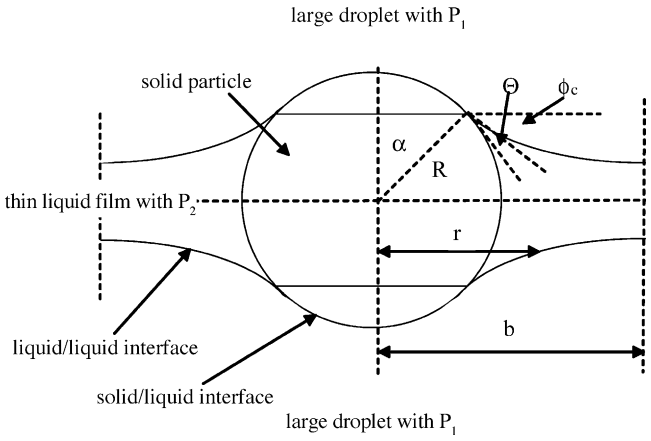

Fig. 1. A solid particle, stabilizing a thin liquid film between two large droplets (illustration for the model of Denkov et al. [43]).

the following integral equation can be written in the dimensionless form (for notations see Fig. 1):

$$\cos(\Theta + \phi_c) = \int_{\sin(\Theta+\phi_c)}^{b*} \frac{b^{*2} - r^{*2}}{[r^{*2}p^{*-2} - (b^{*2} - r^{*2})^2]^{1/2}} \mathrm{d}r^* \tag{3a}$$

where

$$p^* = \frac{\sin(\Theta + \phi_c)\sin\phi_c}{b^{*2} - \sin^2(\Theta + \phi_c)} \tag{3b}$$

with parameter p^*, defined as (see also Eq. (2)):

$$p^* \equiv \frac{RP_c^{max}}{2\sigma} \tag{3c}$$

Parameter p^* was calculated at some selected values of the contact angle, and was plotted as function of parameter b^* (see Fig. 3 of [43]). When the expression for p^* from Eq. (3b) is substituted into Eq. (3a), at any fixed values of parameters Θ and b^* the value of ϕ_c can be numerically calculated by solving Eq. (3a). Substituting this value back into Eq. (3b), the requested value of parameter p^* can be obtained. This procedure was performed numerically in the present work for the large number of parameter combinations Θ and b^*. For those parameter combinations, calculated also in the original paper [43], reasonable agreement was obtained between our results and that of [43].

Based on the numerically calculated values, it was empirically established in this paper that for any fixed value of parameter b^*, the calculated value of parameter p^* appears to be strictly proportional[2] to the cosine of the equilibrium contact angle:

$$p^* = p\cos\Theta \tag{3d}$$

Substituting Eq. (3d) into Eq. (3c), the equation for P_c^{max} can be expressed in the following general form, being valid for the

[1] The Author regrets, that having been familiar mostly with the metallurgical literature, he missed paper [43] when papers [38,63–65], initiated mainly by the metallic foam community, were prepared.

[2] When the accuracy of the numerical solution is increased, the numerically calculated values become closer and closer to Eq. (3d). However, the present author was not able to prove that Eq. (3d) follows analytically from Eqs. (3a)–(3c).

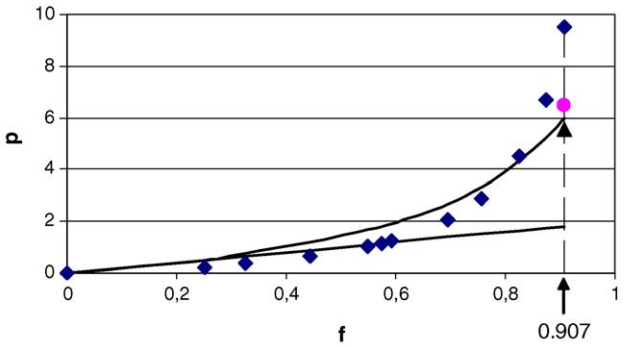

Fig. 2. Dependence of parameter p of Eq. (2a) for a single layer of particles on the interface coverage by particles (rombs [43], calculated in this paper, circle [45], triangle [81], straight line [38], curved line: this paper, Eq. (4h).

single layer of particles:

$$P_c^{\max} = p\frac{2\sigma}{R}\cos\Theta \tag{2a}$$

with parameter p, being a difficult function of parameter b^*. At hexagonal close packing of single layer particles ($b^* = 1.05$ [43]), the numerical solution of Eqs. (3a)–(3c) gives the value: $p = 9.52$. When b^* increases, parameter p rapidly decreases.

For our purposes parameter b^* should be expressed through the interface coverage by the particles (f), as introduced in [38]. Parameter f is defined as the ratio of the projection areas of all the particles at the given interface to the total area of that interface. For the hexagonal close packing of particles $f = 0.907$. At this limit the relationship between the two values can be written simply as: $f = 1/b^{*2}$ (as $0.907 = 1/1.05^2$). However, it should be noted that the two approaches cannot be identical, as a surface cannot be fully covered by circles of equal radii, as follows from model [43]. Nevertheless, parameter p as function of the interface coverage by particles was calculated in the present paper using the relationship $f = 1/b^{*2}$, and plotted in Fig. 2.

2.2. The method of [45]

Visschers et al. [45] studied the closely packed single layer of particles. They derived analogous equations to [43], but approximated the shape of the interface between the three neighboring particles by a segment of the sphere. As a result, they obtained Eq. (2a) with $p = 6.46$ (Fig. 2). One can see that at close packing the results of ($p = 9.52$) [43] and ($p = 6.46$) [45] are different by almost 50%, due to different simplifications, used in the two models (see Fig. 2).

2.3. The method of [38]

In the paper [38], the same Eq. (2a) was derived for the single layer of particles, neglecting the curvature of the liquid/gas interface, and taking into account only the sliding process of the contact line along the spherical particle with an increasing pressure. In this way $p = 2f$ was obtained (see Fig. 2). Thus, at close packing ($f = 0.907$) the value $p = 1.81$ follows, what is considerably lower than the above results. This is obviously due to neglecting the curvature effect.

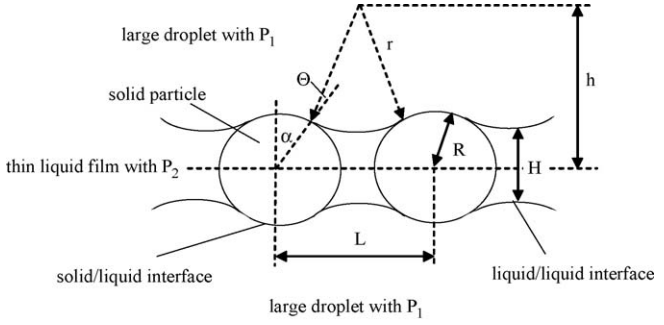

Fig. 3. Schematic of the hexagonally packed single layer of spherical particles, stabilizing the thin liquid film between two large droplets (view from side).

2.4. Extending the method of [45] to hexagonal packing of a single layer of particles

Let us extend the method of [45] to the hexagonal (not close) packing of a single layer of particles in the thin liquid film. First, the case of o/w emulsions and water-based foams will be considered.

Let us consider a hexagonally packed single layer of spherical solid particles at the bubble/liquid/bubble, or drop/liquid/drop interface. The particles have equal sizes of radii R, and the distance between their centers is denoted through L (Fig. 3). The dimensionless distance between the centers of the particles is: $L^* = L/R$. The unit cell of the system (viewed from the top) is a triangle, closed within the lines, connecting the centers of the three neighboring particles. The difference between the pressure in the large drops (P_1) and that in the thin liquid film (P_2) is the capillary pressure ($P_c \equiv P_1 - P_2$). When the capillary pressure is zero, the liquid/liquid interfaces are flat. However, when the capillary pressure is positive, the liquid/liquid interfaces will be curved, as shown in Fig. 3.

The shape of the liquid/liquid interfaces can be described by the Laplace equation, the solution of which is quite difficult for the configuration of three spherical particles. That is why, in this model we will suppose for simplicity that the liquid/liquid interfaces can be described as a segment of a sphere of radius r (see Fig. 3) ($r^* \equiv r/R$). The sphere of radius r will touch each of the three particles at single points, with an angle Θ (the equilibrium contact angle), measured between the radius of the sphere and the radii of the particles at the points of touching (Fig. 3). The center of the sphere will be situated at a certain point, above the center of the triangle, formed by the three particles. The elevation of the central point of the sphere above the plane, formed by the centers of the particles is denoted as h (see Fig. 3) ($h^* \equiv h/R$). From the described geometry, parameters h^* and r^* can be derived as:

$$h^* = \cos\alpha + \left(\frac{L^*}{\sqrt{3}} - \sin\alpha\right) ctg(\alpha - \Theta) \tag{4a}$$

$$r^* = \left(\frac{L^*}{\sqrt{3}} - \sin\alpha\right) \sin^{-1}(\alpha - \Theta) \tag{4b}$$

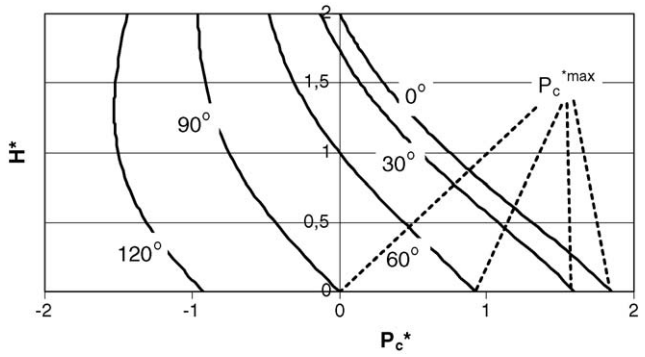

Fig. 4. Dependence of the dimensionless smallest distance between the two, opposing liquid/liquid interfaces as function of the dimensionless capillary pressure for the single layer of particles at $L^* = 2.5$ and selected values of the contact angle (see values on the curves). For any different value of L^* similar graphs can be obtained.

Then, the capillary pressure, corresponding to the given value of the radius of the liquid/liquid interface can be written through the Laplace equation:

$$P_c = \frac{2\sigma}{Rr^*} \tag{4c}$$

Let us define the dimensionless capillary pressure (P_c^*) as:

$$P_c^* \equiv \frac{P_c R}{2\sigma} = \frac{1}{r^*} \tag{4d}$$

The right-hand side of Eq. (4d) follows from the comparison of Eq. (4c) and the definition of P_c^*.

The smallest distance between the two opposing liquid/liquid interfaces is denoted by H in Fig. 3 ($H^* \equiv H/R$). From the geometry of Fig. 3: $H^* = 2(h^* - r^*)$. Substituting Eqs. (4b) and (4c) into this equality, the equation for H^* can be obtained:

$$H^* = 2\cos\alpha + 2\left(\frac{L^*}{\sqrt{3}} - \sin\alpha\right)[ctg(\alpha - \Theta) - \sin^{-1}(\alpha - \Theta)] \tag{4e}$$

At given values of L^* and Θ, the values of H^*, r^* and P_c^* can be calculated as function of parameter α, from Eqs. (4b)–(4e). Thus, from the corresponding values of H^* and P_c^* the dependence of the dimensionless smallest distance between the two, opposing liquid/liquid interfaces can be found as function of the dimensionless capillary pressure. This relationship is shown for some selected values of L^* and Θ in Fig. 4. The following conclusions can be made from Fig. 4:

(i) For the contact angle of $\Theta = 0^\circ$ in the absence of the capillary pressure $H^* = 2$. In other words at $P_c^* = 0$ the particles are situated in the water phase with their full body, with horizontal liquid/liquid interfaces at their top and bottom. At a positive capillary pressure the two liquid/liquid interfaces are gradually pushed towards each other (H^* decreases). At the maximum value of the capillary pressure ($P_c^{*\max}$) H^* becomes zero and the thin liquid film collapses.

(ii) For the contact angle interval $0^\circ < \Theta < 90^\circ$ in the absence of the capillary pressure the liquid/liquid interfaces are planar, but are situated at a closer distance to each other as the contact angle is gradually increased (for example at $P_c^* = 0$ and $\Theta = 60^\circ$: $H^* = 1$). Similarly to the previous case, the distance between the two opposing liquid/liquid interfaces will gradually decrease as the capillary pressure increases, terminating at a certain maximum value of the capillary pressure ($P_c^{*\max}$), at which the thin liquid film collapses due to $H^* = 0$. The value of $P_c^{*\max}$ gradually decreases as the contact angle increases. Nevertheless it means that particles with $0^\circ < \Theta < 90^\circ$ will stabilize o/w emulsions or foams (with a thin water, or liquid film between their cells) at any destabilizing pressure, not exceeding the value of $P_c^{*\max}$.

(iii) For the contact angle of $\Theta = 90^\circ$ in the absence of the capillary pressure $H^* = 0$. In other words the maximum capillary pressure, what the thin liquid film can withstand without collapsing is zero. Thus, single layered particles with $\Theta = 90^\circ$ cannot stabilize o/w emulsions and foams at all.

(iv) At any contact angle $\Theta > 90^\circ$ even in the absence of the capillary pressure H^* has a negative value. It means that such particles will destabilize the o/w emulsions and foams (at least if a single layer of particles is present at the interface), what is a common knowledge in the community [29,73–80].

From the above analysis the algorithm follows to determine the values of the maximum dimensionless capillary pressure ($P_c^{*\max}$). From the condition $H^* = 0$ (see Eq. (4e)) the critical value of parameter α can be found for selected values of L^* and Θ. The analytical expression for the critical sinus value of α follows as:

$$\sin\alpha_{cr} = \frac{-b + \sqrt{b^2 - 4ac}}{2a}, \quad \text{with}$$

$$a = 1 + \frac{L^{*2}}{3} + \frac{2L^*}{\sqrt{3}}\sin\Theta,$$

$$b = -2\left(\frac{L^*}{\sqrt{3}} + \sin\Theta\right)\left(1 + \frac{L^*}{\sqrt{3}}\sin\Theta\right),$$

$$c = \left(\frac{L^*}{\sqrt{3}} + \sin\Theta\right)^2 - \frac{L^{*2}}{3}\cos^2\Theta$$

Substituting this critical value of α into Eqs. (4b)–(4d), the maximum dimensionless capillary pressure is obtained, corresponding to $H^* = 0$, i.e. to the condition of film rupture. Repeating the same procedure for a large number of L^* and Θ values, the dependence of $P_c^{*\max}$ on these parameters is obtained. From the analysis of the obtained set of data it was empirically established that for any value of L^*, $P_c^{*\max}$ is strictly proportional[3] to the cosine of Θ:

$$P_c^{*\max} = p\cos\Theta \tag{4f}$$

[3] Parameter p of Eq. (4f) holds constant with an uncertainty of less than 10^{-8}% at $\Theta < 85^\circ$ (for example, at $L^* = 2$: $p = 6.00000000 = \text{const}$ at any $\Theta < 85^\circ$). As $p \to 0$ at $\Theta \to 90^\circ$, the accuracy of calculation decreases with approaching $\Theta \to 90^\circ$, due to the limitations of the computer (for example, at $L^* = 2$ and $\Theta = 89^\circ$: $p = 5.99999974$, what is different by 4.3×10^{-6}% from $p = 6$). However, similarly to what was said in connection with Eq. (3d), the present Author was not able to prove that Eq. (4f) follows analytically from Eqs. (4a)–(4e).

Taking into account the obvious geometrical relationship $f = 3.628/L^{*2}$, parameter p can be approximately written as function of parameter f as:

$$p \cong 2.1424f - 5.1256f^2 + 28.139f^3 - 44.047f^4 + 27.808f^5 \quad (4h)$$

At hexagonal close packing of single layer of particles ($f = 0.907$): $p = 6.00$. This value is in the middle of the interval, indicated by two other theoretical solutions for the same problem: $p = 5.66$ [81] and $p = 6.46$ [45]. Eq. (4h) is compared to the previous solutions in Fig. 2. From Fig. 2 one can conclude that for all practical purposes Eq. (4h) can serve as the approximated relationship to be used between parameters p and f in Eq. (2a) for the maximum capillary pressure, induced by a single layer of particles in the thin liquid film between bubbles and drops.

The analysis above corresponded to the o/w emulsions (and foams), in which a thin water (liquid) film separates the droplets (bubbles). An analogous derivation can be made for the case of w/o emulsions, in which a thin oil film separates the water droplets. For this latter case all the above equations will be identical, except that the capillary pressure will have an opposite sign. Thus, the most general equation for the maximum capillary pressure for the single layer of particles is written as:

$$P_c^{\max} = \pm p\frac{2\sigma}{R}\cos\Theta \quad (2b)$$

with sign '+', corresponding to the case of o/w emulsions and foams, and sign '−', corresponding to the case of w/o emulsions.

The physical meaning of Eq. (2b) for the single layer of particles in the thin liquid film can be summarized as follows:

(i) emulsions (foams) will be stable only, when the maximum capillary pressure will have a positive value, and if this stabilizing pressure will be stronger, than the sum of all other pressures (due to gravity, or due to centrifugal [82], electric [83] or magnetic [27] fields, etc.), trying to collapse the thin liquid films between the droplets (bubbles);
(ii) o/w emulsions (foams) will be stabilized by the single layer of particles, if the contact angle is lower than 90°; the maximum stabilization corresponding to the contact angle of 0°. The opposite is also true: o/w emulsions (foams) will be de-stabilized by particles, having the contact angle larger than 90°;
(iii) w/o emulsions will be stabilized by the single layer of particles, if the contact angle is higher than 90°; the maximum stabilization corresponding to the contact angle of 180°. The opposite is also true: w/o emulsions will be de-stabilized by particles, having the contact angle lower than 90°.

Now let us make an order of magnitude calculation with Eq. (2b). Let us suppose the following parameters: $f = 0.907$ (closely packed single layer of particles), as a consequence: $p = 6$ (see Eq. (4h)), $\Theta = 70°$, $\sigma = 0.03\ \mathrm{J/m^2}$ (a characteristic interfacial energy for oil/water interfaces). Then, a closely packed single layer of solid spherical particles of radii $R = 10\ \mu\mathrm{m}$ will provide the maximum capillary pressure of 0.123 bar. Compared to the outside pressure, the effect of gravity, possible vibrations during usage and transportation, etc. this capillary pressure obviously will not be sufficient to stabilize o/w emulsions. Indeed, all reports on particle stabilized o/w or w/o emulsions mention submicron, or maximum micron-sized particles, which are actually able to stabilize emulsions (see [15,16] and references thereof). When the radii of the solid particles are decreased to 10 nm, the maximum capillary pressure increases to 123 bar under the same conditions. Such a high stabilizing pressure ensures a virtually ever-lasting emulsion under normal conditions, supposing the liquid phases are not evaporated, or destroyed in other ways.

The second parameter, being able to ensure high stability of foams or emulsions, is the interfacial energy, as follows from Eq. (2b). When the interfacial energy is increased 30 times compared to an example above ($0.9\ \mathrm{J/m^2}$ is close to the surface tension of liquid aluminum), the maximum stabilizing pressure, calculated by Eq. (2b) increases to 3.69 bar even for large particles $R = 10\ \mu\mathrm{m}$. This maximum capillary pressure is sufficient to stabilize liquid aluminum foams,[4] despite the unexpected (for the o/w community) size of the stabilizing particles. This prediction of Eq. (2b) is in accordance with experimental observations (see [14] and references thereof).

2.5. The joint analysis of Eq. (1) with Eq. (2b)

It can be seen that the conclusions, made after Eqs. (1) and (2b), are partly excluding each other. However, both Eqs. (1) and (2b) should provide as high (positive) values as possible to ensure emulsion (foam) stability. An analysis, being similar to this joint analysis of Eqs. (1) and (2b) was first performed in [38].

Let us denote by ε_p the probability that under equal other circumstances (same size of particles and same interfacial energy) the solid particles will be stabilized at the liquid/liquid interface. As follows from Eq. (1): $\varepsilon_p = (1 \pm \cos\Theta)^2$. The probability ε_p as function of the contact angle is shown in Fig. 5a. As follows from Fig. 5a, the particles will be situated at the liquid/liquid or liquid/gas interface with the highest probability at $\Theta = 90°$.

Now, let us denote by ε_{w-fl} the probability that under equal other circumstances (same size of particles, same interfacial energy and same coverage of the interface by particles) the thin water (liquid) film between the oil droplets (gas bubbles) will be stabilized by a single layer of particles. As follows from Eq. (2b): $\varepsilon_{w-fl} = \cos\Theta$. Similarly, the probability that under equal other circumstances the thin oil film between the water droplets will be stabilized by a single layer of particles is written as: $\varepsilon_{o-fl} = -\cos\Theta$. These two probabilities as function of the contact angle are shown in Fig. 5b. As follows from Fig. 5b, the thin water (liquid) film between the oil droplets (gas bubbles) will be most stable at $\Theta = 0°$, while the thin oil film between the water droplets will be most stable at $\Theta = 180°$.

[4] It should be mentioned that metallic foams should be stable in liquid state only for a short period of time during their production, as they are used in solid state, only after their solidification.

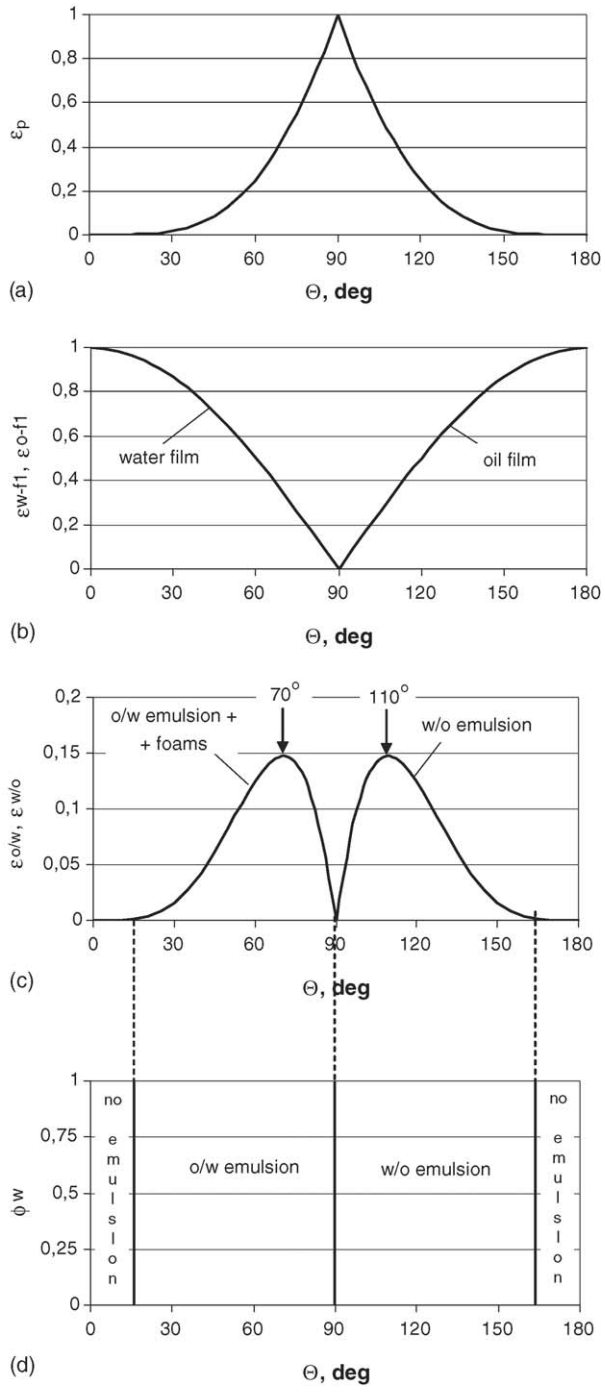

Fig. 5. The probabilities that the particles are stabilized at the liquid/liquid or liquid/gas interface (a), that the liquid films are stabilized by a single layer of particles (b), and that the emulsions (foams) are stabilized at $\phi_w = 0.5$ (c). The emulsion stability diagram for a single layer of stabilizing particles (d).

Let us denote by ε the probability of the complex event that both the particles at the interface and the thin liquid films will be stable under the same conditions. For the equal volume ratios of water and oil phases this complex probability ε will be proportional to the probability that a given type of emulsion under given circumstances is stable. Thus, the stability of o/w emulsions (foams) will be proportional to: $\varepsilon_{o/w} = \varepsilon_p \varepsilon_{w-f1}$. Similarly, the stability of w/o emulsions will be proportional to: $\varepsilon_{w/o} = \varepsilon_p \varepsilon_{o-f1}$. These two complex probabilities are shown in Fig. 5c as function of contact angle. As follows from Fig. 5c, the optimum contact angle for the formation of o/w emulsions (foams) is about 70°, while that for the formation of w/o emulsions is about 110°. This is in perfect agreement with experimental observations [8,26,39–42].

Based on Fig. 5c, the 'emulsion stability diagram' (ESD) can be constructed (see Fig. 5d). The ESD shows the regions of stable emulsion types as function of water volume fraction (ϕ_w) and contact angle. As the contact angle intervals with positive values of $\varepsilon_{o/w}$ and $\varepsilon_{w/o}$ do not overlap in Fig. 5c, the stability regions of w/o and o/w emulsions will not be functions of the water content of the emulsion. That is why, a straight vertical line separates the stability ranges of o/w and w/o emulsions in Fig. 5d. As one can see from Fig. 5d, o/w emulsions (foams) are stable in the contact angle interval of $15° < \Theta < 90°$, while the w/o emulsion is stable at $90° < \Theta < 165°$. It should be mentioned that this conclusion is valid only for the single layer of stabilizing particles in the thin liquid film between the droplets or bubbles.

As one can see from the ESD of Fig. 5d, an o/w emulsion can be converted into a w/o emulsion or vice-versa only by changing the contact angle through the value of 90°. However, as one can see from Fig. 5c, at this contact angle of 90° both emulsion types have zero stability. Therefore, catastrophic phase inversion in emulsions cannot be explained by the single layer of stabilizing particles.

3. Equations for P_c^{max} for a closely packed double layer of particles

Eq. (2b) and the ESD, presented in Fig. 5d, have only one drawback: they are not able to explain the experimental observation that water based [42] or metallic [84] foams can be somewhat stable even when the contact angle is larger than 90°. As was already presented [38], these observations can be explained only by supposing the presence of a double layer of closely packed particles, or other, multi-layer configurations. This is also in accordance with other observations [47] that double or multiple layers of particles are able to stabilize emulsions regardless of their contact angle (see also [85]). As will be shown below, the hypothesis on the double layer of particles will also lead to a logical explanation of the catastrophic inversion of emulsions from o/w type into w/o type (and back) solely by changing the volume fraction of the water phase.

If two droplets, both fully covered by particles approach each other, the natural consequence of their approach is the formation of a closely packed double layer of particles in the thin liquid film between the two large droplets. Such a schematic picture was first shown in papers of Tambe and Sharma (see Fig. 11 [25] or Fig. 1 in [86]). This idea was converted into the model for the maximum capillary pressure first by Nushtayeva and Kruglyakov [55], and later by the present author [38]. Although this configuration is probably not widely spread in real emulsions and foams, it is worth to model, as it can be considered as a transition between the single layer of particles (see previous chapter) and the 3D network of particles (see next chapter). Detailed modeling of the closely packed double layer

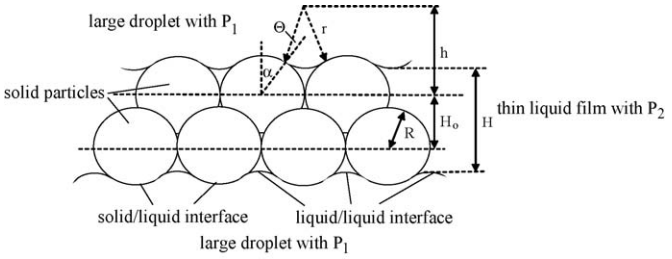

Fig. 6. Schematic of the closely packed double layer of spherical particles, stabilizing the thin liquid film between two large droplets ($H_o = 1.633R$).

of particles is important, as the 3D network of particles has a less definite structure, and thus, cannot be properly modeled. Hence, the model to be developed in this chapter should be considered as the pre-requisite to model the 3D network of particles.

3.1. The method and results of Nushtaeva and Kruglyakov [55]

In their first three papers on the subject, Nushtaeva and Kruglyakov [55,57,59] derived the equation for the capillary pressure for the closely packed double layer of particles. Similarly to [45], the shape of the liquid/liquid interface between the particles was described as a part of a sphere of radius r (Fig. 6). The capillary pressure was described as function of angle α (Fig. 6) [55,57,59]:

$$P_c(\alpha) = \frac{2\sigma}{R}\frac{\cos[\Theta + (90 - \alpha)]}{1.1547 - \cos(90 - \alpha)} \tag{5a}$$

The maximum capillary pressure was defined at $\alpha = 90^\circ$ [55,57] (see Fig. 6). Substituting this value into Eq. (5a), the following equation was obtained for the maximum capillary pressure (see Eq. (5a) and (5) of [57])[5]:

$$P_c^{\max} = \frac{2\sigma}{R}\frac{\cos\Theta}{0.1547} \tag{5b}$$

One can see that Eq. (5b) is identical with Eq. (2a), with $p = 6.46$. This result is identical with that of [45], what seems to be unexpected, as in [45] a single layer, while in [55] a double layer of closely packed particles were considered. It is quite obvious that in reality the solutions to these two cases should be different (see also [85]). The reason for this unexpected result is that Nushtaeva and Kruglyakov [55,57,59] used an incorrect boundary condition for the film rupture in the case of the double layers of particles ($\alpha = 90^\circ$, see Fig. 6 and [61]). As will be shown below, this condition provides a correct result only at $\Theta = 0^\circ$ (see Fig. 8 for comparison).

3.2. The method and results [38]

For the closely packed double layer of particles in the thin liquid film between large bubbles the following expression was derived by the author [38]:

$$P_c^{\max} = p\frac{2\sigma}{R}(\cos\Theta + z) \tag{2c}$$

where $p = 2f$ (as above for the single layer of particles [38]); z, a constant, depending on the arrangement of particles in the thin liquid film. For the single layer of particles $z = 0$ and Eq. (2c) reduces to Eq. (2a). For the closely packed double layer of particles $z = 0.633$ [38].

Eq. (2c) was successfully applied [38] to explain observations on stabilization of thin liquid films, even if the contact angle is larger than 90° [42,84].

It should be recognized, however, that Eq. (2c) is in conflict with Eq. (5b), developed by Nushtayeva and Kruglyakov [55] for the closely packed double layer of particles (see footnote to paper [62]). The main reason for this discrepancy is the inadequate choice of the boundary condition by [55,57] (see above and [61]). On the other hand, it should also be recognized that Eq. (2c) was derived [38] in a simplified way, neglecting the curvature of the liquid/gas interface. That is why, the formalism, developed in Section 2.4 for the case of the double layer of closely packed particles will be applied here to check whether Eq. (2c) is adequate, or not.

3.3. The maximum capillary pressure, acting on the spherical segment of a liquid/liquid interface in the closely packed double layer of spherical particles

Fig. 6 applies to this situation. First, let us consider the case of o/w emulsions and water foams, with a thin water layer between the droplets and bubbles.

The equations for dimensionless parameters h^* and r^*, described earlier by Eqs. (4a) and (4b) will remain valid, except that they are simplified due to the case of closely packed particles, by taking $L^* = 2$:

$$h^* = \cos\alpha + \left(\frac{2}{\sqrt{3}} - \sin\alpha\right) ctg(\alpha - \Theta) \tag{6a}$$

$$r^* = \left(\frac{2}{\sqrt{3}} - \sin\alpha\right) \sin^{-1}(\alpha - \Theta) \tag{6b}$$

The smallest distance between the opposing liquid/liquid interfaces can be calculated in dimensionless coordinates from Fig. 6 as: $H^* = H_o^* + 2(h^* - r^*)$. From the geometry of the closely packed systems the distance between the two planes, formed by the centers of neighboring particle planes: $H_o^* = 1.633$. Substituting into this equation Eqs. (6a) and (6b), the following equation is obtained:

$$H^* = 1.633 + 2\cos\alpha + 2\left(\frac{L^*}{\sqrt{3}} - \sin\alpha\right) \times [ctg(\alpha - \Theta) - \sin^{-1}(\alpha - \Theta)] \tag{6c}$$

A simplest condition for film rupture is: $H^* = 0$. However, as follows from the theoretical analysis of penetration of liquids into closely packed system of equal spheres [89–91] (see also [92,93]), the capillary pressure curve will go through a maximum

[5] Eq. (5b) is rewritten in the latest papers of the authors [62,87] with misprints [88].

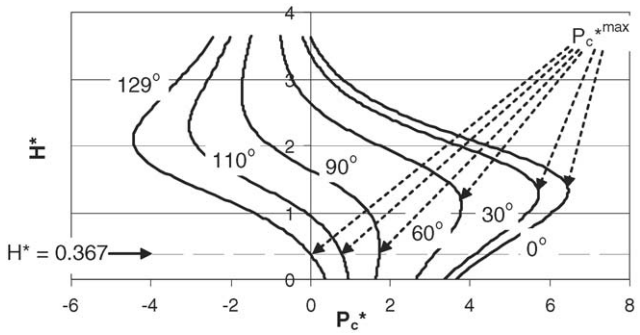

Fig. 7. The dependence of the smallest dimensionless distance between the opposing liquid/liquid interfaces as function of dimensionless pressure for the closely packed double layer of particles at different values of the contact angle (figures at the curves).

point, when the liquid/liquid interface, penetrating into the pores between the top layer of the particles reaches the top of the second layer of particles, situated in the bottom row. From simple geometry of the three-dimensional double layer of closely packed particles one can see that it will happen when the penetration depth equals $(8/3)^{1/2}R = 1.633R$ [89–91]. This means that the smallest distance between the two opposing liquid/liquid interfaces must be as low as $2R + 1.633R - 2{\cdot}1.633R = 0.367$R. Thus, the real condition of film rupture is: $H^* = 0.367$.

The dimensionless distance between the tops of two particle layers is 3.633. Therefore, let us plot the H^* value as function of the dimensionless capillary pressure (defined by Eqs. (4c) and (4d)) in the interval between $H^* = 0$ and $H^* = 3.633$ for the case of the closely packed double layer of particles at different contact angle values (Fig. 7). The following conclusions can be made from Fig. 7:

(i) For the contact angle of $\Theta = 0°$ in the absence of the capillary pressure $H^* = 3.633$. In other words at $P_c^* = 0$ all the particles are situated in the water phase with their full body, with a horizontal liquid/liquid interfaces at the top of the top layer and at the bottom of the bottom layer of particles. When the capillary pressure is gradually increased, the two liquid/liquid interfaces are gradually pushed towards each other (H^* decreases). At a certain value of H^* (being above 0.367) the capillary pressure goes through a maximum value, meaning that there is no further pressure needed to push the two opposing liquid/liquid interfaces towards each other—once this maximum value is reached, the thin liquid film will inevitably collapse. That is why this maximum value corresponds to the requested value of $P_c^{*\max} = 6.46$. This value coincides with the solution of [55] only for $\Theta = 0°$.

(ii) For the contact angle interval $0° < \Theta < 90°$ at $P_c^* = 0$ the liquid/liquid interfaces are planar, but are situated at a closer distance to each other as the contact angle is gradually increased (for example at $P_c^* = 0$ and $\Theta = 60°$: $H^* = 2.633$). Similarly to the previous case, the distance between the two opposing liquid/liquid interfaces will gradually decrease as the capillary pressure increases, and at a certain value of H^* (being above 0.367) the capillary pressure goes through a maximum value, what is the requested $P_c^{*\max}$. This $P_c^{*\max}$ value gradually decreases as the contact angle increase from 0° to 90°.

(iii) For the contact angle of $\Theta = 90°$ at $P_c^{*\max} = 0$: $H^* = 1.633$. A certain positive interval of capillary pressures exist, at which $H^* > 0.367$, and so the double layer of closely packed particles can stabilize the thin film also at $\Theta = 90°$, what makes this case qualitatively different from that of the single layer of particles. One can also see from Fig. 7 that the maximum value of the capillary pressure is reached exactly at $H^* = 0.367$. Thus, the way to determine the maximum capillary pressure changes when the contact angle is larger than 90°.

(iv) In the contact angle interval $129.3° > \Theta > 90°$ the thin liquid film still can be stabilized by the double layer of particles, as a certain positive interval of capillary pressures exist, which ensure $H^* > 0.367$. In this case the value of $P_c^{*\max}$ is found from the interception of the $H^* - P_c^*$ curve with the value of $H^* = 0.367$.

(v) For the contact angle of $\Theta = 129.3°$ at $P_c^* = 0$: $H^* = 0.367$, what is the condition for film rupture. It means that for this contact angle $P_c^* = 0$. Thus, for the double layer of closely packed particles $\Theta = 129.3°$ is the critical contact angle, above which this arrangement of particles is not able to stabilize the thin liquid film between the droplets or bubbles. An analogous critical contact angle ($50.7° = 180° - 129.3°$) was found also from the penetration studies [89–91].

(vi) At any contact angle above 129.3° the capillary pressure will be negative for any value $H^* > 0.367$. Consequently the double layer of particles with this contact angle interval will be destabilizing o/w emulsions (foams).

Based on the above analysis and Fig. 7, the dimensionless maximum capillary pressure was determined for different values of the contact angle (see Fig. 8). The plotted values are reasonably close to the experimental values of dimensionless break-through pressures, determined in [55,94]. The difference between the theoretical and experimental curves is due to the

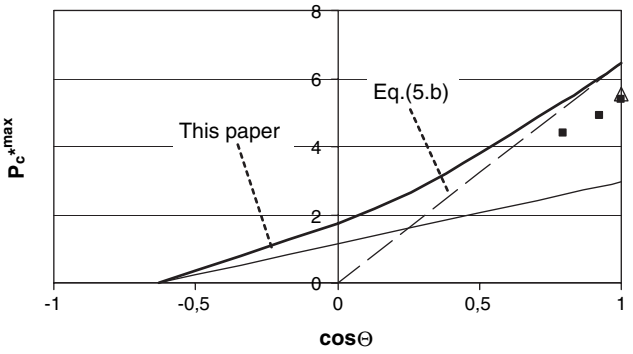

Fig. 8. The dependence of the dimensionless maximum capillary pressure on the cosine of the contact angle for the closely packed double layer of particles (bold solid line: numerical values, calculated in this paper, broken line: theoretical values, calculated in [55], thin solid line: theoretical values, calculated in [38], triangle: experimental point of [94], squares: experimental data of [55]).

spherical simplification of the shape of the liquid/liquid interface. One can see that our new solution at $\Theta = 0^\circ$ coincides with that of [55], while at 129.3° it coincides with our previous, simplified solution [38].

From Fig. 8 one can see that there is a break-point at our calculated curve at $\cos\Theta = 0$ (i.e. $\Theta = 90^\circ$), what follows from the two different types of conditions, applied to find the maximum capillary pressure below and above 90° (see above). As a consequence, the curve in Fig. 8 can be described only in two different parts by the following semi-empirical equations:

$$P_c^{*\max} = 4.27(\cos\Theta + 0.405) \quad \text{(simplified equation at } \Theta < 90^\circ) \tag{6d}$$

$$P_c^{*\max} = 3.49(\cos\Theta + 0.361\cos^2\Theta + 0.486) \quad \text{(more exact equation at } \Theta < 90^\circ) \tag{6e}$$

$$P_c^{*\max} = 2.73(\cos\Theta + 0.633) \quad (\text{valid at } \Theta \geq 90^\circ) \tag{6f}$$

As one can see from Eqs. (6d) and (6f), they are of the same form as Eq. (2c) [38], with somewhat different numerical coefficients.

The above analysis is valid for the o/w emulsions (foams), with a thin water (liquid) film between the droplets (bubbles). When the stability of w/o emulsions is considered, an analogous derivation can be presented, but with a mirror reflection of our curve in Fig. 8 around the value of $\Theta = 90^\circ$. Thus, Eqs. (6d)–(6f) are transformed for the case of w/o emulsions as:

$$P_c^{*\max} = -4.27(\cos\Theta - 0.405) \quad \text{(simplified equation at } \Theta > 90^\circ) \tag{6g}$$

$$P_c^{*\max} = -3.49(\cos\Theta - 0.361\cos^2\Theta - 0.486) \quad \text{(more exact equation at } \Theta > 90^\circ) \tag{6h}$$

$$P_c^{*\max} = -2.73(\cos\Theta - 0.633) \quad (\text{valid at } \Theta \leq 90^\circ) \tag{6i}$$

If only the simplified Eqs. (6d), (6f), (6g) and (6i) are considered, the general equation for the maximum capillary pressure can be written as:

$$P_c^{\max} = \pm p\frac{2\sigma}{R}(\cos\Theta \pm z) \tag{2d}$$

with a '+' sign, referring to o/w emulsions (foams), and with a '−' sign referring to w/o emulsions.

One can see that Eq. (2d) is a more general form of Eqs. (2b) and (2c). The values of parameters p and z for different particle arrangements and contact angle intervals are collected in Table 1.

Table 1
The values of parameters p and z of Eq. (2d) for different cases

Situation Parameter	Single layer $\Theta \leq 90^\circ$	cp double layer $\Theta < 90^\circ$ (o/w) $\Theta > 90^\circ$ (w/o)	cp double layer $90^\circ \leq \Theta \leq 129.3^\circ$ (o/w) $50.7^\circ \leq \Theta \leq 90^\circ$ (w/o)
p	Eq. (4h)	4.27	2.73
z	0	0.405	0.633

3.4. The joint analysis of Eq. (1) with Eq. (2d) for the double layer of particles

Now let us perform an analysis, being similar to Fig. 5 for the double layer of particles (see Fig. 9). For the high stability of solid particles stabilized emulsions and foams, both Eqs. (1) and (2d) should provide positive, and as high as possible values.

Similarly to Section 2.5, let us denote by ε_p the probability that under equal circumstances (same size of particles and same interfacial energy) the solid particles will be stabilized at the liquid/liquid interface. As follows from Eq. (1): $\varepsilon_p = (1 \pm \cos\Theta)^2$. Fig. 9a is identical with Fig. 5a.

Now, let us denote by ε_{w-f2} the probability that under equal other circumstances (same size of particles, same interfacial energy) the thin water (liquid) film between the oil droplets (gas bubbles) will be stabilized by a double layer of closely packed particles. As follows from Eq. (2d): $\varepsilon_{w-f2} = p(\cos\Theta + z)/6$ (division by 6 is for normalization purposes, values of parameters p and z are collected in Table 1 for different contact angle intervals). Similarly, the probability that under equal other circumstances the thin oil film between the water droplets will be stabilized by a double layer of closely packed particles is written as: $\varepsilon_{o-f2} = -p(\cos\Theta - z)/6$. These two probabilities as function of the contact angle are shown in Fig. 9b. As follows from Fig. 9b, the thin water (liquid) film between the oil droplets (gas bubbles) will be most stable at $\Theta = 0^\circ$, while the thin oil film between the water droplets will be most stable at $\Theta = 180^\circ$. So far, these conclusions have been identical to those, drawn from Fig. 5b. However, Fig. 9b is essentially different from Fig. 5b. The main difference is that the stability intervals of the water and oil thin films overlap in Fig. 9b (in the interval of $50.7^\circ < \Theta < 129.3^\circ$), while these two intervals are fully separated in Fig. 5b. As was shown above, this difference is mainly due to the 3D nature of the double layer of particles, compared to the 2D nature of the single layer of particles.

Let us denote by ε the probability of the complex event that both the particles at the interface and the thin liquid films will be stable under the same conditions. For the equal volume ratios of water and oil phases this complex probability ε will be proportional to the probability that a given type of emulsion under given circumstances is stable. Thus, the stability of o/w emulsions (foams) will be proportional to: $\varepsilon_{o/w} = \varepsilon_p\varepsilon_{w-f2}$. Similarly, the stability of w/o emulsions will be proportional to: $\varepsilon_{w/o} = \varepsilon_p\varepsilon_{o-f2}$. The particular expressions for the complex probabilities ε are given in Table 2. These two complex probabilities are shown in Fig. 9c as function of contact angle. As follows from Fig. 9c, the optimum contact angle for the formation of o/w emulsions (foams) is about 86°, while that for the formation of w/o emulsions is about 94°. This is still in agreement with the experimentally observed optimum contact angle interval [8,26,39–42].

As a consequence of the overlapping curves in Fig. 9b, the curves in Fig. 9c overlap, as well. Thus, both o/w and w/o emulsions are somewhat stable in the contact angle interval of

Table 2
Particular expressions for the complex probability ε (see Table 1 and Fig. 9c)

Θ-interval	$\Theta \leq 90^\circ$	$\Theta \geq 90^\circ$
$\varepsilon_{o/w}$	$4.27(1-\cos\Theta)^2 \times (\cos\Theta + 0.405)$	$2.73(1+\cos\Theta)^2 \times (\cos\Theta + 0.6.33)$
$\varepsilon_{w/o}$	$-2.73(1-\cos\Theta)^2 \times (\cos\Theta - 0.633)$	$-4.27(1+\cos\Theta)^2 \times (\cos\Theta - 0.405)$

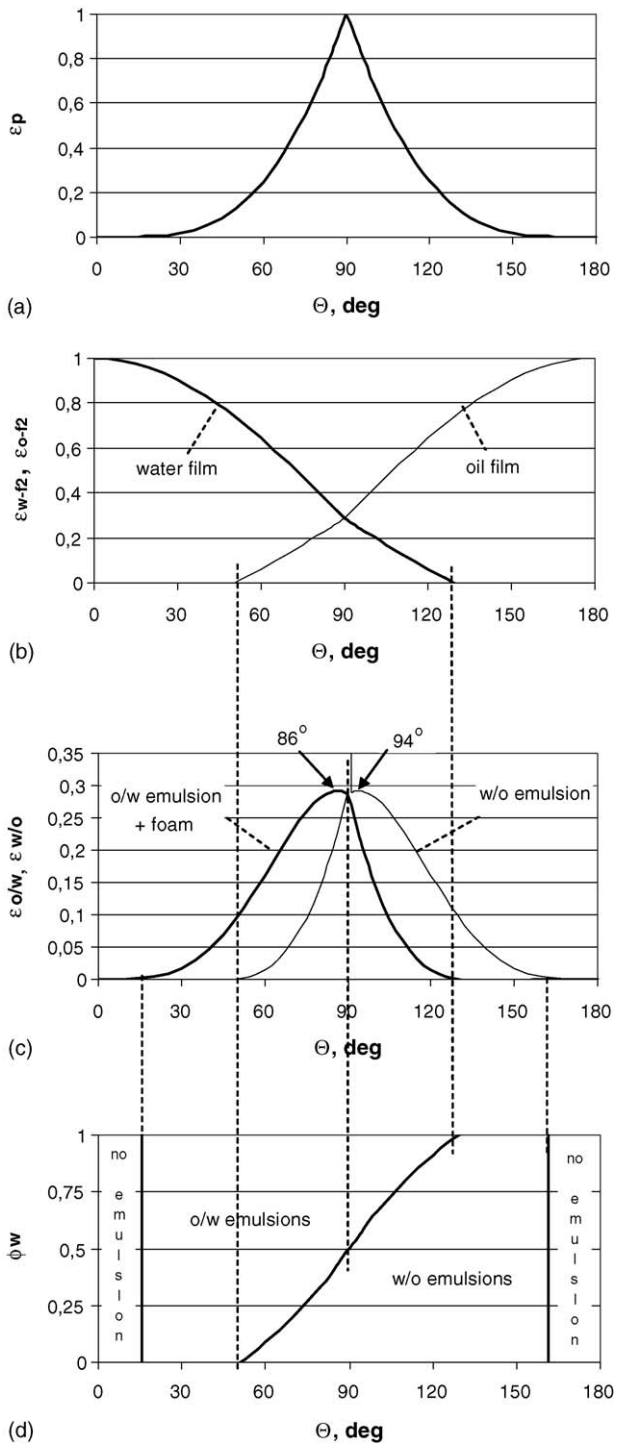

Fig. 9. The probabilities that the particles are stabilized at the liquid/liquid or liquid/gas interface (a), that the liquid films are stabilized by a double layer of closely packed particles (b), and that the emulsions (foams) are stabilized at $\phi_w = 0.5$ (c). The emulsion stability diagram for a double layer of closely packed, stabilizing particles (d).

$50.7^\circ < \Theta < 129.3^\circ$. As a result, the emulsion stability diagram for the double layer of closely packed particles (Fig. 9d) will be more complex than for the single layer of particles (Fig. 5d). What can be stated for sure is that in the contact angle interval $15^\circ < \Theta < 50.7^\circ$ the o/w emulsion will be stable, as only the thin water film is stable in this interval, while the thin oil film is not stable at all (see Fig. 9b–d). Similarly one can state with confidence that in the contact angle interval $129.3^\circ < \Theta < 165^\circ$ the w/o emulsion will be stable, as only the thin oil film is stable in this interval, while the thin water film is not stable at all (see Fig. 9b–d).

The most difficult task in constructing the emulsion stability diagram (Fig. 9d), is to determine the preferential emulsion type (o/w or w/o) in the contact angle interval of $50.7^\circ < \Theta < 129.3^\circ$ (as function of water content), where both emulsion types are somewhat stable. In order to find the proper equation, let us consider first some obvious boundary conditions:

(i) As the stability probabilities ε of Fig. 9c correspond to the equal volume fractions of water and oil, the formation probabilities of o/w and w/o emulsions will be obviously equal, if $\varepsilon_{w/o} = \varepsilon_{o/w}$ and if $\phi_w = 1 - \phi_w = 0.5$. Also, at $\phi_w = 1 - \phi_w = 0.5$ the o/w emulsion will be preferred, if $\varepsilon_{w/o} < \varepsilon_{o/w}$ (i.e. at $\Theta < 90^\circ$) and vice versa.

(ii) At $\Theta = 50.8^\circ$ (i.e. just a little above the critical value of 50.7°), the stability of the water film around oil droplets is much more stable than that of the oil film around the water droplets. Such a large difference in thin film stability cannot be compensated by the water or oil content of the emulsion. As a consequence, at $\Theta = 50.8^\circ$ the oil drops, separated by thin water films will be preferentially stable at virtually any value of φ_w, i.e. the preferential emulsion type will be o/w.

(iii) At $\Theta = 129.2^\circ$ (i.e. just a little below the critical value of 129.3°), the stability of the oil film around water droplets is much more stable than that of the water film around the oil droplets. Such a large difference in thin film stability cannot be compensated by the water or oil content of the emulsion. As a consequence, at $\Theta = 129.2^\circ$ the water drops, separated by thin oil films will be preferentially stable at virtually any value of φ_w, i.e. the preferential emulsion type will be w/o.

The above boundary conditions will be satisfied, if the following conditions are fulfilled:

$$\text{preferential o/w emulsion, if : } (1-\phi_w)\varepsilon_{w/o} < \phi_w \varepsilon_{o/w} \quad (7a)$$

$$\text{preferential w/o emulsion, if : } (1-\phi_w)\varepsilon_{w/o} > \phi_w \varepsilon_{o/w} \quad (7b)$$

In accordance with Eqs. (7a) and (7b), the equation of the line, separating the preferentially o/w emulsion region from the preferentially w/o emulsion region, can be written as:

$$(1-\phi_w)\varepsilon_{w/o} = \phi_w \varepsilon_{o/w} \quad (7c)$$

It should be mentioned that in principle there are many other mathematical equations, which would formally satisfy the above boundary conditions. However, Eqs. (7a)–(7c) seem to be the simplest equations among all the possible ones, and therefore, these equations will be preferred to construct the emulsion stability diagram for the double layer of closely packed particles, in the first approximation.

If the equations, presented in Table 2 are substituted into equality (7c), the critical volume fraction of the water phase can be expressed as function of contact angle. Then, the following two equations can be obtained for the curved line in Fig. 9d:

$$\phi_{w,cr} = \left(1 + 1.56 \cdot \frac{\cos\Theta + 0.405}{0.633 - \cos\Theta}\right)^{-1} \quad (\text{at } 50.7^\circ < \Theta < 90^\circ) \quad (7d)$$

$$\phi_{w,cr} = \left(1 + 0.639 \cdot \frac{\cos\Theta + 0.633}{0.405 - \cos\Theta}\right)^{-1} \quad (\text{at } 90^\circ < \Theta < 129.3^\circ) \quad (7e)$$

3.5. On the explanation of the catastrophic phase inversion in solid particle stabilized emulsions

In Fig. 10, the emulsion stability diagram for emulsions, stabilized by the double layer of closely packed particles is redrawn from Fig. 9d. The arrows in the diagram indicate the possible routes of catastrophic phase inversions due to gradually increasing or decreasing the water content of the emulsion in the same three-phase (water/oil/solid) system. According to Fig. 10, the catastrophic phase inversion is expected to be a reversible process. For example, if the contact angle is 100°, the w/o emulsion will be stable at $\phi_w < 0.66$, and the o/w emulsion will be stable at $\phi_w > 0.66$. It is interesting to note that at this contact angle value both the w/o and o/w emulsions are quite stable (compare with Fig. 9c).

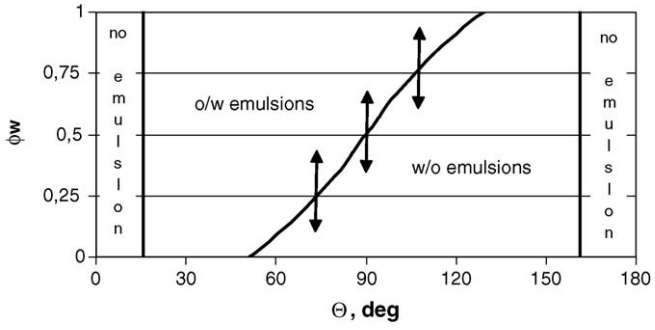

Fig. 10. The emulsion stability diagram for emulsions, stabilized by the double layer of closely packed particles. The arrows indicate possible routes for catastrophic phase inversions by changing the water content of the emulsion.

A phenomenon of catastrophic phase inversion by changing the water content of emulsion was found experimentally by Binks and Lumsdon [50,77,95]. Reviewing the results of these experiments, Binks [15] and later Aveyard et al. [16] concluded: 'it remains to understand why both types of emulsion occur in systems containing the same three components (oil, water, solid)'. The present author believes that the emulsion stability diagram, presented in Fig. 10 provides a reasonable explanation. However, it should be mentioned that contact angle values on experimentally used nano-particles are not known [50,77,95], and so the agreement between the experimental results and Fig. 10 is confirmed only qualitatively. We would like to note that a different explanation for the same phenomenon was offered recently by Kralchevsky et al. [37].

Another type of catastrophic phase inversion is predicted in Fig. 11. Let us first consider an emulsion with $\phi_w = 0.1$, $\Theta = 75^\circ$, and with such a small amount of solid particles, what is able to cover the thin films only by a monolayer (or less). Then, Fig. 11a applies, and o/w emulsion will form. Now, let us add solid particles into the system in an amount, being sufficient to cover all thin films by a closely packed double layer (or by a 3D network of particles, see below). Then, Fig. 11b applies, and the original o/w emulsion is expected to invert into a w/o emulsion (see LHS arrow between Fig. 11a and b). This process is expected to be reversible.

Similarly, let us consider the emulsion with $\phi_w = 0.9$, $\Theta = 105^\circ$, and with such a small amount of solid particles, what is able to cover the thin films only by a monolayer (or less).

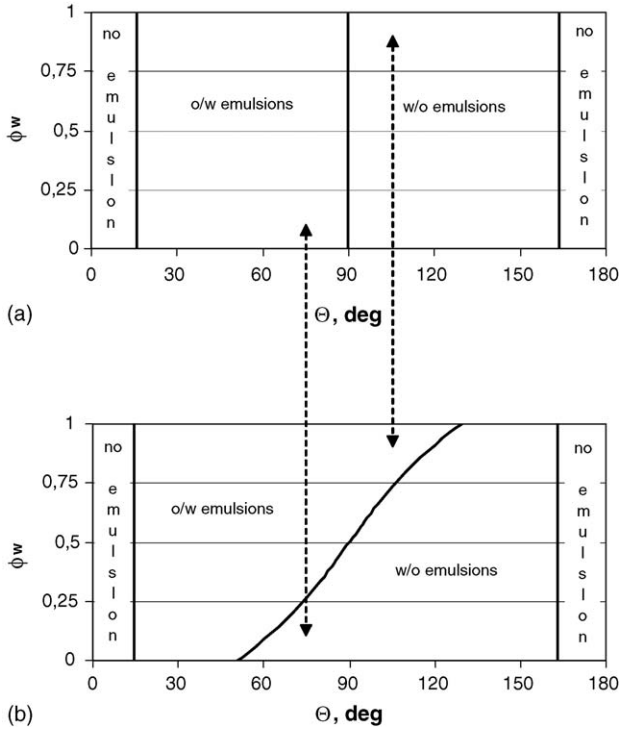

Fig. 11. The stability diagram of emulsions of the single layer of particles (a) and for the closely packed double layer of particles (b) in the thin liquid film between large droplets. Arrows show possible routes of catastrophic phase inversions due to the increase (or decrease) of the solid particle content in the emulsion.

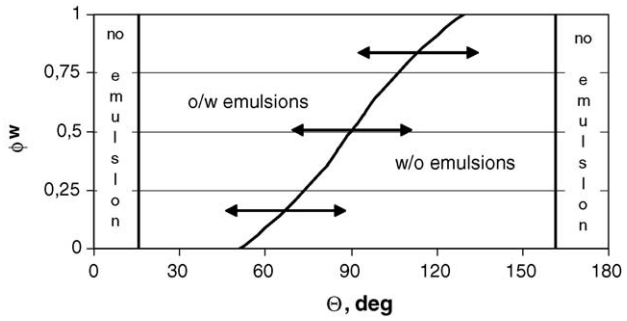

Fig. 12. The emulsion stability diagram for emulsions, stabilized by the double layer of closely packed particles. The arrows indicate possible routes for transitional phase inversions by changing the hydrophobic character of the particles.

Then, Fig. 11a applies, and a w/o emulsion will form. Now, let us add solid particles into the system in an amount, being sufficient to cover all thin films by a closely packed double layer (or by a 3D network of particles – see below). Then, Fig. 11b applies, and the original w/o emulsion is expected to invert into an o/w emulsion (see RHS arrow between Fig. 11a and b). This process is expected to be reversible, as well.

The results of similar, but different set of experiments were published recently by Binks et al. [96] with an equal volume of oil and water phases ($\phi_w = 0.5$). Unfortunately, the phase inversion at this water content cannot be rationalized by the emulsion stability diagram of Fig. 11.

3.6. On the explanation of the transitional phase inversion in solid particle stabilized emulsions

In Fig. 12, the emulsion stability diagram for emulsions, stabilized by the double layer of closely packed particles is redrawn from Fig. 9d. The arrows in the diagram indicate the possible routes of transitional phase inversions due to gradually increasing or decreasing the value of the contact angle. It can be achieved by changing the composition of the liquid phases, or by changing the ratio of the hydrophobic to hydrophilic particles [97]. This process is expected to be reversible. As follows from Fig. 12, the emulsion stability diagram predicts that the critical ratio of hydrophobic to hydrophilic particles, needed for transitional phase inversion from o/w emulsion into w/o emulsion, will be higher for higher water content of the emulsion. Unfortunately, no experimental information has been found to check, if this hypothesis is correct, or not. It should be reminded, that this hypothesis is valid only, if the emulsion is stabilized by a double layer of closely packed particles. In case of a single layer of particles, the critical ratio of hydrophobic to hydrophilic particles, needed for transitional phase inversion from o/w emulsion into w/o emulsion, will not depend on the water content of the emulsion (see Fig. 5d).

4. The case of the 3D network of particles in the thin liquid film

It has been repeatedly reported in the literature of emulsions and foams that the formation of 3D networks of particles (flocculation) increases the stability of emulsions and foams [15,30,47–50,60,98–108]. STXM images of 3D networks between droplets are presented in [109] (see also scanning electron microscopy images [110]). Most of the authors rightly point out that the increase of macroscopic viscosity might be one of the reasons for the enhanced stability of emulsions (on the rheology of emulsions see [111]). However, it should be reminded that the microscopic (true) viscosity of the liquid in the pores of the 3D network of particles remains very low, and so the coalescence of droplets in principle can take place by the penetration of the droplets towards each other through those pores. The only primary reason why it is not taking place is the capillary pressure, stabilizing the thin liquid film in the pores of the 3D network of particles. The first model for the maximum capillary pressure for the 3D network of particles was presented by the author [38].

For the case of the 3D network of particles also Eq. (2d) will be valid, with the maximum possible value of $z = 1$, as was predicted earlier [38]. In reality, there is a distribution of arrangements of particles in the 3D network, what makes exact modeling very difficult. The distribution of the particle arrangements will lead to the distribution of the values of both parameters p and z. Parameter p will have a positive value, and will be a function of coverage of the two liquid/liquid interfaces by particles. Parameter z mostly will be determined by the position of the second row of particles next to the one, attached to the liquid/liquid interface. Thus, the distribution of different values of parameter z between 0 and 1 will take place at different places of the emulsion. As for the closely packed double layer of particles parameter z is around 0.5 (see Tables 1 and 2), in the first approximation Fig. 9d, developed for the closely packed double layer of particles, can also be considered as the 'average' stability diagram for the case of 3D network of particles. The line, representing the boundary between o/w and w/o emulsions in Fig. 9d will obviously cross the point $(90^\circ - 0.5)$ also for the 3D network of particles, but might extend more along the contact angle axes, compared to Fig. 9d. In other words, emulsions and foams, stabilized by a 3D network of particles, can be stable even at contact angles, being higher than 129.3° (for o/w emulsions and foams) and at contact angles, being lower than 50.7° (for w/o emulsions). Thus, foams and emulsions, stabilized by the 3D network of particles, can be stable virtually at any contact angle. A similar conclusion follows from some experimental papers [47,60,84].

Fig. 9d (and Figs. 10–12) can also be used as an 'average' stability diagram for the interpretation of catastrophic and transitional phase inversions of emulsions, if the thin liquid layers between the droplets are stabilized by 3D network of particles.

5. Conclusions

(i) It has been shown that in addition to the energy of particle removal from the liquid/liquid interface (Eq. (1)), the maximum capillary pressure (introduced by Denkov et al. [43]) should also be taken into account for the analysis of the emulsions stability by solid particles (Eq. (2)).
(ii) The general Eq. (2d) with Table 1 was derived, to describe the maximum capillary pressure for different particle arrangements.

(iii) Eqs. (1) and (2d) were jointly analyzed for the case of the single layer of particles (Fig. 5) and for the case of the closely packed double layer of particles (Fig. 9). The joint interval of optimum contact angles of stabilization of emulsions and foams by a single or a closely packed double layer of particles appears to be between 70° and 86° (for the o/w emulsions and foams), and between 94° and 110° (for the w/o emulsions).

(iv) If the emulsion (foam) is stabilized by a single layer of solid particles, o/w emulsions and foams will be stable at $15^\circ < \Theta < 90^\circ$, while the w/o emulsion are stable at $90^\circ < \Theta < 165^\circ$.

(v) If the emulsion (foam) is stabilized by a double layer of solid particles, o/w emulsions and foams will be stable at $15^\circ < \Theta < 129.3^\circ$, while the w/o emulsion will be stable at $50.7^\circ < \Theta < 165^\circ$. As these intervals overlap, the line, separating the o/w emulsion from the w/o emulsion will be a curve in the coordinates of contact angle–water content (see Eqs. (7d) and (7e) and Fig. 9d).

(vi) Reversible catastrophic phase inversion by changing solely the water content of emulsion is explained by the emulsion stability diagram (Fig. 10).

(vii) Reversible catastrophic phase inversion is predicted by changing solely the particle concentration for the case of unequal volume fractions of water and oil (see Fig. 11).

(viii) Transitional phase inversion by changing the ratio of hydrophobic to hydrophilic particles is explained by the emulsion stability diagrams. When the thin liquid films are stabilized by a single layer of particles, the critical ratio of different particles will not depend on the water content of emulsion (see Fig. 5d). However, when the thin liquid films are stabilized by the closely packed double layer of particles, the critical ratio of hydrophobic to hydrophilic particles will increase by increasing the water content of the emulsion (see Fig. 12).

(ix) If the emulsion (foam) is stabilized by a 3D network of solid particles, Fig. 9d (and Figs. 10–12) can be used as an 'average' emulsion stability diagram. However, in this case the curved line, separating the o/w emulsion region from the w/o emulsion region might be somewhat different from that, shown in Fig. 9d, and might depend on the actual structure of the 3D network. This question should be addressed in more details in the future.

References

[1] W. Ramsden, Proc. R. Soc. 72 (1903) 156.
[2] S.U. Pickering, J. Chem. Soc. 91 (1907) 2001.
[3] W.D. Bancroft, J. Phys. Chem. 16 (1912) 475.
[4] F.R. Newman, J. Phys. Chem. 18 (1914) 34.
[5] T.R. Briggs, J. Ind. Eng. Chem. 13 (1921) 1008.
[6] P. Finkle, H.D. Draper, J.H. Hildebrand, J. Am. Chem. Soc. 45 (1923) 2780.
[7] A.J. Scarlett, W.L. Morgan, J.H. Hildebrand, J. Phys. Chem. 31 (1927) 1566.
[8] J.H. Schulman, J. Leja, Trans. Faraday Soc. 50 (1954) 598.
[9] R. Aveyard, J.H. Clint, J. Chem. Soc. Faraday Trans. 91 (1995) 2681.
[10] H.D. Goff, Int. Dairy J. 7 (1997) 363.
[11] P.M. Kruglyakov, Hydrophile–Lipophile Balance of Surfactants and Solid Particles, Elsevier Science, Amsterdam, 2000.
[12] D. Rousseau, Food Res. Int. 33 (2000) 3.
[13] V. Gergely, H.P. Degischer, T.W. Clyne, in: T.W. Clyne (Ed.), Comprehensive Composite Materials, vol. 3, Elsevier Science Ltd., 2000, p. 797.
[14] J. Banhart, Prog. Mater. Sci. 46 (2001) 559.
[15] B.P. Binks, Curr. Opin. Colloid Interface Sci. 7 (2002) 21.
[16] R. Aveyard, B.P. Binks, J.H. Clint, Adv. Colloid Interface Sci. 100–102 (2003) 503.
[17] B.S. Murray, R. Ettelaie, Curr. Opin. Colloid Interface Sci. 9 (2004) 314.
[18] P. Kruglyakov, A. Nushtaeva, in: D.N. Petsev (Ed.), Emulsions: Structure and Interactions, Elsevier, 2004, p. 641 (Chapter 16).
[19] A.F. Koretzki, P.M. Kruglyakov, Izv. Sib. Otd. AN SSSR, seriia khim. nauk, No. 2, vip. 1 (1971) 139.
[20] A. Scheludko, B.V. Toshev, D.T. Bojadjiev, J. Chem. Soc. Faraday Trans. I 72 (1976) 2815.
[21] T.F. Tadros, B. Vincent, in: P. Becher (Ed.), Encyclopedia of Emulsion Technology, vol. 1, Dekker, New York, 1983, p. 130 (Chater 3).
[22] S. Levine, B.D. Bowen, S.J. Patridge, Colloids Surf. 38 (1989) 325.
[23] J.H. Clint, S.E. Taylor, Colloids Surf. 65 (1992) 61.
[24] D.E. Tambe, M.M. Sharma, J. Colloid Interface Sci. 157 (1993) 244.
[25] D.E. Tambe, M.M. Sharma, Adv. Colloid Interface Sci. 52 (1994) 1.
[26] N. Yan, J.C. Masliyah, Colloids Surf. A: Physicochem. Eng. Aspects 96 (1995) 229.
[27] S. Melle, M. Lask, G.G. Fuller, Langmuir 21 (2005) 2158.
[28] B.P. Binks, J.A. Rodrigues, Angew. Chem. Int. Ed. 44 (2005) 441.
[29] R. Aveyard, B.P. Binks, P.D.I. Fletcher, C.E. Rutherford, J. Dispersion Sci. Technol. 15 (1994) 251.
[30] B.P. Binks, S.O. Lumsdon, Phys. Chem. Chem. Phys. 1 (1999) 3007.
[31] Z. Hórvölgyi, M. Máté, A. Dániel, J. Szalma, Colloids Surf. A: Physicochem. Eng. Aspects 156 (1999) 501.
[32] Gy. Tolnai, F. Csempesz, M. Kabai-Faix, E. Kálmán, Zs. Keresztes, A.L. Kovács, J.J. Ramsden, Z. Hórvölgyi, Langmuir 17 (2001) 2683.
[33] V.B. Menon, R. Nagarajan, D.T. Wasan, Sep. Sci. Technol. 22 (1987) 2295.
[34] S. Levine, B.D. Bowen, Colloid Surf. 59 (1991) 377.
[35] J. Drelich, Colloids Surf. A: Physicochem. Eng. Aspects 116 (1996) 43.
[36] R. Aveyard, J.H. Clint, T.S. Horozov, Phys. Chem. Chem. Phys. 5 (2003) 2398.
[37] P.A. Kralchevsky, I.B. Ivanov, K.P. Ananthapadmanabhan, A. Lips, Langmuir 21 (2005) 50.
[38] G. Kaptay, Colloids Surf. A: Physicochem. Eng. Aspects 230 (2003) 67.
[39] P.M. Kruglyakov, A.F. Koretzki, Izv. Sib. Otd. AN SSSR, ser. khim. nauk, No. 9, vip. 4 (1971) 16.
[40] G. Johansson, R.J. Pugh, Int. J. Miner. Proc. 34 (1992) 1.
[41] S.W. Ip, Y. Wang, J.M. Toguri, Can. Metall. Q. 38 (1999) 81.
[42] Y.Q. Sun, T. Gao, Metall. Mater. Trans. 33A (2002) 3285.
[43] N.D. Denkov, I.B. Ivanov, P.A. Kralchevsky, D.T. Wasan, J. Colloid Interf. Sci. 150 (1992) 589.
[44] J.-P. Hsu, B.-T. Liu, J. Phys. Chem. B 101 (1997) 5147.
[45] M. Visschers, J. Laven, R. van den Linde, Prog. Org. Coat. 31 (1997) 311.
[46] K.P. Velikov, F. Durst, O.D. Velev, Langmuir 14 (1998) 1148.
[47] S. Abend, N. Bonnke, U. Gutschner, G. Lagaly, Colloid Polym. Sci. 276 (1998) 730.
[48] G. Lagaly, M. Reese, S. Abend, Appl. Clay Sci. 14 (1999) 83.
[49] J. Thieme, S. Abend, G. Lagaly, Colloid Polym. Sci. 277 (1999) 257.
[50] B.P. Binks, S.O. Lumsdon, Langmuir 16 (2000) 2539.
[51] F.L. Roman, M. Schmidt, H. Lowen, Phys. Rev. E 61 (2000) 5445.
[52] J. Sur, H.K. Pak, J. Korean Phys. Soc. 38 (2001) 582.
[53] J. Sur, H.K. Pak, Phys. Rev. Lett. 86 (2001) 4326.
[54] J.-P. Hsu, J.-H. Lu, Y-C. Kuo, S. Tseng, Colloid Surf. B 21 (2001) 265.
[55] A.V. Nushtayeva, P.M. Kruglyakov, Mendeleev Commun. (2001) 235.

[56] K.-L. Gosa, V. Uricanu, Colloids Surf. A: Phychem. Eng. Aspects 197 (2002) 257.
[57] A.V. Nushtayeva, P.M. Kruglyakov, Colloid J. 65 (2003) 341.
[58] E.J. Stancik, M. Kouhkan, G.G. Fuller, Langmuir 20 (2004) 90.
[59] P.M. Kruglyakov, A.V. Nushtayeva, Adv. Colloid Interface Sci. 108–109 (2004) 151.
[60] S. Simovic, C.A. Prestidge, Langmuir 20 (2004) 8357.
[61] T.S. Horozov, R. Aveyard, J.H. Clint, B. Neumann, Langmuir 21 (2005) 2330.
[62] P.M. Kruglyakov, A.V. Nushtayeva, Colloids Surf. A: Physicochem. Eng. Aspects 263 (2005) 330.
[63] G. Kaptay, in: J. Banhart, M.F. Ashby, N.A. Fleck (Eds.), Metal Foams and Porous Metal Structures, MIT Verlag, Bremen, 1999, p. 141.
[64] G. Kaptay, in: J. Banhart, M.F. Ashby, N.A. Fleck (Eds.), Cellular Metals and Metal Foaming Technology, MIT Verlag, Bremen, 2001, p. 117.
[65] G. Kaptay, in: J. Banhart, N.A. Fleck, A. Mortensen (Eds.), Cellular metals: Manufacture, Properties, Applications, MIT Verlag, Bremen, 2003, p. 107.
[66] C. Körner, M. Arnold, R.F. Singer, Mater. Sci. Eng. A396 (2005) 28.
[67] V.B. Menon, A.D. Nikolov, D.T. Wasan, J. Colloid Interface Sci. 124 (1988) 317.
[68] M. Szekeres, O. Kamalin, P.G. Grobet, R.A. Schoonheydt, K. Wostyn, K. Clays, A. Persoons, I. Dékány, Colloids Surf. A: Physicochem. Eng. Aspects 227 (2003) 77.
[69] K.D. Danov, B. Pouligny, P.A. Kralchevsky, Langmuir 17 (2001) 6599.
[70] S. Tarimala, L.L. Dai, Langmuir 20 (2004) 3492.
[71] Z. Hórvölgyi, S. Németh, J.H. Fendler, Langmuir 12 (1996) 997.
[72] B.R. Midmore, Colloids Surf. A: Physicochem. Eng. Aspects 132 (1998) 257.
[73] P.R. Garret, J. Colloid Interface Sci. 69 (1979) 107.
[74] A. Dippenaar, Int. J. Miner. Process. 9 (1982) 1.
[75] D.E. Tambe, M.M. Sharma, J. Colloid Interface Sci. 171 (1995) 463.
[76] R.J. Pugh, Adv. Colloid Interface Sci. 64 (1996) 67.
[77] B.P. Binks, S.O. Lumsdon, Phys. Chem. Chem. Phys. 2 (2000) 2959.
[78] K.G. Marinova, N.K. Denkov, P. Branlard, Y. Giraud, M. Deruelle, Langmuir 18 (2002) 3999.
[79] N.D. Denkov, Langmuir 20 (2004) 9463.
[80] J. Legrand, M. Chamerois, F. Placin, J.E. Poirier, J. Bibette, F. Leal-Calderon, Langmuir 21 (2005) 64.
[81] G. Mason, N.R. Morrow, J. Colloid Interface Sci. 168 (1994) 130.
[82] S. Tcholakova, N.D. Denkov, I.B. Ivanov, B. Campbell, Langmuir 18 (2002) 8960.
[83] A.P. Sullivan, P.K. Kilpatrick, Ind. Eng. Chem. Res. 41 (2002) 3389.
[84] T. Wübben, S. Odenbach, Colloids Surf. A: Physicochem. Eng. Aspects 266 (2005) 207.
[85] S.E. Friberg, J. Dispersion Sci. Technol. 26 (2005) 647.
[86] D.E. Tambe, M.M. Sharma, J. Colloid Interface Sci. 162 (1994) 1.
[87] P.M. Kruglyakov, A.V. Nushtayeva, N.G. Vilkova, J. Colloid Interface Sci. 276 (2004) 465.
[88] P.M. Kruglyakov: personal e-mail, sent to the author on 09.09.2005.
[89] G. Kaptay, D.M. Stefanescu, AFS Trans. 100 (1992) 707.
[90] G. Kaptay, Mater. Sci. Forum 414–415 (2003) 419.
[91] T. Bárczy, G. Kaptay, Mater. Sci. Forum 473–474 (2005) 297.
[92] G. Kaptay, J. Mater. Sci. 40 (2005) 2125.
[93] G. Kaptay, T. Bárczy, J. Mater. Sci. 40 (2005) 2531.
[94] G. Mason, N. Morrow, J. Colloid Interface Sci. 109 (1986) 46.
[95] B.P. Binks, S.O. Lumsdon, Langmuir 16 (2000) 8622.
[96] B.P. Binks, J. Philip, J.A. Rodrigues, Langmuir 21 (2005) 3296.
[97] B.P. Binks, S.O. Lumsdon, Langmuir 16 (2000) 3748.
[98] A.F. Koretzki, A.B. Taubman, Abh. Dtsch. Akad. Wiss. Berlin, Kl. Chem. Geol. Biol. 6 (1967) 676.
[99] A. Tsugita, S. Takemoto, K. Mori, T. Yoneya, Y. Otani, J. Colloid Interface Sci. 95 (1983) 551.
[100] V.B. Menon, D.T. Wasan, Sep. Sci. Technol. 19 (1984) 555.
[101] H. Hassander, B. Johansson, B. Törnell, Colloid Surf. 40 (1989) 93.
[102] K. Boode, P. Walstra, Colloids Surf. A: Physicochem. Eng. Aspects 81 (1993) 121.
[103] K. Boode, P. Walstra, Colloids Surf. A: Physicochem. Eng. Aspects 81 (1993) 139.
[104] S. Puskás, J. Balázs, A. Farkas, I. Regdon, O. Berkesi, I. Dékány, Colloids Surf. A: Physicochem. Eng. Aspects 113 (1996) 279.
[105] N.P. Ashby, B.P. Binks, Phys. Chem. Chem. Phys. 2 (2000) 5640.
[106] N. Babcsán, D. Leitlmeier, H.P. Degischer, Mat. wiss. U. Werkstofftech. 34 (2003) 1.
[107] R.G. Alargova, D.S. Warhadpande, V.N. Paunov, O.D. Velev, Langmuir 20 (2004) 10371.
[108] M.D. Eisner, H. Wildmoser, E.J. Windhab, Colloids Surf. A: Physicochem. Eng. Aspects 263 (2005) 390.
[109] U. Neuhausler, S. Abend, C. Jacobsen, G. Lagaly, Colloid Polym. Sci. 277 (1999) 719.
[110] B.P. Binks, M. Kirkland, Phys. Chem. Chem. Phys. 4 (2002) 3727.
[111] H.A. Barnes, in: D.N. Petsev (Ed.), Emulsions: Structure and Interactions, Elsevier, 2004, p. 721 (Chapter 18).